GAMMA-2 Scientific Workshop on the Emission of Prompt Gamma Rays in Fission and Related Topics

Shape-isomer studies with resonance neutron capture

A. Dragić[a,**], G. Nyman[b], A. Oberstedt[b], S. Oberstedt[a]

[a] *European Commission, DG Joint Research Centre (IRMM), 2440 Geel, Belgium*
[b] *Fundamental Fysik, Chalmers Tekniska Högskola, 41296 Göteborg, Sweden*

Abstract

An experiment searching for formation of super-deformed shape isomers in odd uranium isotopes following neutron capture is designed at the GELINA neutron source of IRMM. We focus on neutron energies around the so-called intermediate structure in the fission cross-section, where the coupling between compound states above the first and the second minimum is largest. The experimental arrangement is described. The results of a feasibility study on the population of the shape isomer in ^{235}U, using a ^{234}U target, together with the results from first run with a ^{238}U target are presented.

1. Introduction

Introduction of microscopic shell corrections into macroscopic liquid drop model (Strutinski V.M., 1967) led to the picture of doubly-humped barrier in actinide nuclear binding energy. The concept successfully explained intermediate structure in sub-threshold fission cross sections as well as the existence of shape isomers.

Many research effort since 1960s resulted in the discovery of various shape isomers and in the characterization of their fission barriers. A (relatively) recent review lists 35 shape isomers (Singh et al., 2002). However, data for shape isomers of odd-N uranium isotopes are still lacking. Since the pioneering work on ^{239}U of Oberstedt and Gunsing (Oberstedt and Gunsing, 1998) and on ^{235}U of Oberstedt et al. (Oberstedt et al., 2007) no new results are published. It is our intention to study shape isomers of ^{239}U and ^{235}U by means of (n, γ) reaction. We plan to investigate the γ-decay of the shape isomer back to the normal ground state by γ-spectroscopic methods. In order to study the feasibility of our concept we conducted two test experiments with the two named uranium isotopes, and the results are presented in this paper.

---

* On leave from Institute of Physics, Pregrevica 118, Belgrade, Serbia.
** Corresponding author.
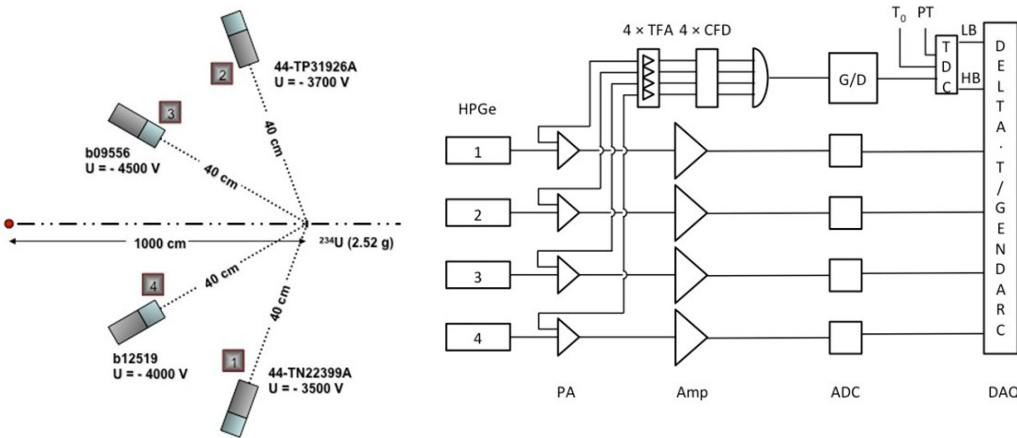*E-mail address:* aleksandar.dragic@ec.europa.eu

Fig. 1. (a) Detector setup and; (b) data acquisition system.

2. Experimental details

Both the ^{234}U and ^{238}U measurements are performed at the GELINA pulsed white energy neutron source of the Institute for Reference Materials and Measurements (IRMM) in Geel, Belgium. The host measurement station is at 10 m nominal distance from the neutron production target. Our detector system consists of four n-type coaxial HPGe detectors of 45% relative efficiency. Two detectors are produced by (Canberra, 2007) and two by (Ortec, 2004). All detectors are electrically cooled. The energy resolution at E_γ = 1332.5 keV (^{60}Co) ranges from 2.1-2.4 keV, measured with 2μs shaping time.

The data acquisition system is based on a *Delta-T* data-acquisition (DAQ) system (Send GmbH, 2000) and the GENDARC on-/off-line data analysis software, which was developed at IRMM (Figure 1). One output from the detector preamplifier (PA) is used to determine the amplitude of the signal. After amplification and shaping (Amp) the signal is digitized (ADC) and fed into the DAQ. The second PA output is used for obtaining the neutron time-of-flight information. The signal is fed into a timing filter amplifier (TFA) and constant fraction discriminator (CFD) for accurate timing. During the feasibility study timing problems were enhanced due to noise, appearing with the frequency of the linac electron beam.

For neutron time-of-flight (TOF) determination we use the signal, t_0, which comes from the electron burst just before impinging on the mercury-cooled uranium target used for neutron production, as start signal. The stop signal is generated from any HPGe detector which has registered an event. The difference of both signals is the TOF, from which the neutron energy may be calculated. To avoid the γ-flash triggering the DAQ a 10μs anti-coincidence gate following the t_0 signal is applied.

3. Results

3.1. ^{234}U run

Experimental setup for the ^{234}U run has been described in the previous section and schematically represented on Fig. 1. The experiment has been performed in the frame of the EUFRAT trans-national access programme at IRMM (Eufrat, 2011). The ^{234}U target was a 3.0 cm disc made from 2.1285(1) g of ^{234}U (99.077%, ^{235}U: 0.076%, ^{236}U: 0.057%, ^{238}U: 0.79%). The major difficulty in the experiment stems from the high intrinsic activity of the target (5.8×10^8 Bq). Total count rate in the detector system is 10^4 cps, even in beam-off condition. With the neutron beam on the target the experimental spectrum is still dominated by the target activity, arising mainly from the presence of the isotope ^{232}U with $T_{1/2}$ = 68 y and, therefore, very high specific activity. Two isotopes from ^{232}U decay chain are

Table 1. List of observed neutron resonances in the ^{234}U time-of-flight spectrum. The two resonances at 59 and 142.2 eV could not be attributed to any isotope present in the target or set-up, yet.

TOF (μs)	$E_n(eV)$ (calibrated)	$E_n(eV)$ (tabulated value)	TOF (μs)	$E_n(eV)$ (calibrated)	$E_n(eV)$ (tabulated value)
144.4	29.5	31.13	61.5	187.8	187.52
116.5	46.4	48.56	58.0	214.0	208.4
106.2	59.0	-	55.8	233.8	237.8
93.2	75.0	77.38	53.2	261.1	258.3
84.9	91.9	94.29	49.9	302.6	307.5
80.2	103.9	106.13	46.1	363.2	359.1
78.5	108.9	111.06	43.6	416.3	412.6
69.8	142.2	-	42.9	431.8	436.3
69.0	144.8	146.25	40.8	485.9	489.0
67.7	151.1	152.16	40.0	511.9	511.0
63.2	176.1	176.18	39.4	529.9	526.2
62.4	181.5	182.49			

responsible for the majority of γ-lines in the spectrum: ^{208}Tl and ^{212}Po. Observed γ-lines from these two isotopes are listed here:

^{208}Tl :   485.95 keV, 510.77 keV, 583.19 keV, 650.10 keV, 763.13 keV, 821.20 keV, 860.56 keV,
              927.60 keV, 982.60 keV, 1093.90 keV, 1282.80 keV, 1592.5 keV, 2103.51 keV, 2614.51 keV.
^{212}Po :   727.33 keV, 893.39 keV, 952.12 keV, 1078.63 keV, 1109.7 keV,
              1512.8 keV, 1620.74 keV, 1679.45 keV, 1806.0 keV.

In the time-of-flight spectrum resonant structures are observed and attributed to capture resonances in ^{234}U (see Table 1). In addition to the tabulated ^{234}U resonances, two resonances at energies 59 eV and 142 eV are observed in the time-of-flight spectrum.

Although resonances are present, spectra produced with cuts on resonant part of TOF curve does not differ significantly from spectra obtained from the non-resonant part. Prospects for observation of shape isomer population are not favourable without allowing for longer measurement time and without setup improvement.

3.2. ^{238}U run

A test measurement with ^{238}U target was performed for a live time of 320270 s. The target is a disk of 11.1 cm radius, made from depleted uranium (0.2% of ^{235}U). Four HPGe detectors are arranged similarly as in the ^{234}U run, at 40 cm distance from the target. Two detectors are positioned at 90$^{\rm o}$ and the two others at 115$^{\rm o}$ with respect to the neutron beam. Recorded spectra are highly complex, with more than 200 γ-lines arising from natural background, radiation from the target, and neutron-induced radiation in the accelerator wall, detectors or other materials present in the laboratory. A summary of all γ-lines identified in the spectrum together with the corresponding count rate is given below. Some lines which should be present in the spectra but were not found are indicated as "below detection limit" (below DL).

3.2.1. Radiation from the target

^{234m}Pa :   258.2 keV (0.44 cps), 742.8 keV (0.84 cps), 766.4 keV (3.12 cps), 921.7 keV (below DL),
              1001.03 keV (4.98 cps), 1237.3 keV (0.30 cps), 1737.7 keV (0.11 cps),1831.5 keV (0.07 cps),
              1867.7 keV (0.06 cps), 1875.5 keV (0.04 cps).
^{234}Pa :   569.3 keV (below DL), 926.4 keV (0.14 cps).

3.2.2. Environmental radiation

^{238}U decay chain (other than ^{234m}Pa and ^{234}Pa)

^{214m}Bi :   609.3 keV(below DL), 665.5 keV(0.04 cps), 806.2 keV(below DL), 1120.3 keV(0.62 cps),
     1377.7 keV (below DL), 1408.0 keV (0.15 cps), 1764.5 keV (0.63 cps),1847.4 keV (0.02 cps),
     2204.2 keV (0.33 cps), 2447.9 keV (0.1124 cps).
   ^{214}Pb :   351.9 keV(below DL).

^{232}Th decay chain

^{228m}Ac :   338.3 keV(0.60 cps), 726.9 keV(below DL), 755.3 keV (0.10 cps), 795.0 keV (0.21 cps)
     911.2 keV (0.91 cps), 969.0 keV(0.54 cps), 1588.2 keV(below DL),1630.6 keV (0.05 cps).
^{212}Pb :   238.6 keV (2.44 cps).
^{212}Bi :   727.2 keV(below DL), 1620.6 keV(below DL).
^{208}Tl :   277.4 keV (0.85 cps), 583.2 keV (1.24 cps), 860.6 keV (0.21 cps), 2614.5 keV (1.01 cps).

^{40}K: 1460.8 keV (6.08 cps)

3.2.3. Neutron induced radiation

In detectors.   Many γ-lines arising from neutron capture on Ge isotopes are visible, but not lines from neutron inelastic scattering, indicating absence of fast neutrons in the fly path. Lines from ^{115}In(n, γ) reaction are found in Ortec detectors only.

^{73}Ge(n, γ) :   492.9 keV (1.01 cps), 595.9 keV(8.10 cps), 608.4 keV (below DL), 638.8 keV (0.03 cps),
     701.5 keV (0.31 cps), 867.9 keV (2.50 cps), 961.05 keV(below DL), 1033.1 keV (0.02 cps),
     1131.4 keV (0.16 cps), 1204.2 keV (1.41 cps), 1267.7 keV (0.04 cps), 1471.6 keV (0.16 cps),
     1489.3 keV (0.11 cps), 1942.0 keV (below DL), 2073.7 keV (0.12 cps), 2368.2 keV (0.02 cps).

^{70}Ge(n, γ) :   283.3 keV (0.16 cps), 391.4 keV (0.24 cps), 500.0 keV (4.22 cps), 708.1 keV (1.95 cps),
     747.1 keV (0.51 cps), 808.1 keV (below DL), 831.3 keV (1.07 cps), 1026.4 keV (0.09 cps),
     1095.5 keV(below DL), 1096.1 keV(below DL), 1139.2 keV (0.70 cps), 1298.6 keV (0.89 cps),
     1378.7 keV(below DL), 1416.0 keV (0.07 cps), 1598.5 keV (0.31 cps), 1743.4 keV (0.07 cps),
     1965.0 keV (0.29 cps), 2032.7 keV (0.09 cps), 2351.0 keV (0.14 cps), 2534.4 keV (0.12 cps),
     2675.8 keV (0.06 cps).

^{72}Ge(n, γ) :   297.2 keV (2.83 cps), 1250.1 keV (0.05 cps).

^{74}Ge(n, γ) :   253.0 keV (2.34 cps), 575.0 keV (0.66 cps), 632.4 keV (0.32 cps), 2138.7 keV (0.01 cps).

^{115}In(n, γ) :   272.9 keV (0.47 cps), 385.1 keV (0.13 cps), 416.9 keV (1.42 cps), 818.6 keV (0.27 cps),
     1293.4 keV (1.81 cps), 2112.1 keV (0.44 cps), 2390.1 keV (0.20 cps), 2801.0 keV (0.04 cps).

In concrete walls.   Typical concrete contains oxygen, silicon, hydrogen, calcium, aluminium, magnesium, iron etc. In accelerator walls, neutron shielding materials, such as boron are also present. Some of the most intense γ-lines in the spectrum are generated in neutron interactions with wall material.

^{28}S$i(n, \gamma)$:   1273.3 keV(below DL), 1867.3 keV(below DL), 2092.9 keV(below DL), 2425.5 keV (0.04 cps).

^{1}H$(n, \gamma)d$:   1711.9 keV (0.81 cps), 2223.1 keV (10.39 cps).

^{40}Ca(n, γ) :   1942.6 keV(below DL), 2001.6 keV (0.11 cps), 2009.8 keV (0.09 cps).

^{27}Al(n, γ) :   983.0 keV (0.16 cps), 1013.7 keV (0.09 cps), 1526.1 keV (0.06 cps), 1778.6 keV (4.61 cps), 2271.6 keV (0.05 cps), 2282.7 keV (0.10 cps), 2577.7 keV (0.06 cps), 2590.0 keV (0.09 cps), 2821.9 keV(0.0858cps).

^{56}Fe(n, γ) :   352.4 keV(below DL), 366.7 keV (0.26 cps), 569.9 keV (below DL), 692.0 keV (0.80 cps), 884.7 keV (0.32 cps), 898.3 keV (0.37 cps), 920.8 keV (below DL), 1019.0 keV (0.32 cps), 1197.3 keV (below DL), 1358.7 keV (0.09 cps), 1612.8 keV (0.57 cps), 1674.6 keV (0.02 cps), 1810.5 keV (0.25 cps), 2066.2 keV (0.17 cps), 2091.8 keV(below DL), 2129.5 keV (below DL), 2721.2 keV (0.10 cps).

^{10}B$(n, \alpha)^7Li$ 477.7 keV (52.62 cps)

In other lab material. Among other materials found in the laboratory, noticeable contribution to spectrum comes from cadmium, used as overlap filter, and chlorine, since certain amounts of PVC are always present.

^{113}Cd(n, γ) :   558.4 keV (2.85 cps), 1364.3 keV (0.13 cps),1660.4 keV (0.09 cps), 2660.1 keV (0.04 cps).

^{35}Cl(n, γ) :   786.3 keV(below DL), 788.4 keV (below DL), 1164.8 keV (0.86 cps), 1951.1 keV(below DL), 1959.3 keV(below DL), 2863.8 keV (0.12 cps).

3.3. Coincidences

A time-to-amplitude converter was operated between detectors 3 and 4 (cf. Figure 1). Lines present in summed spectrum with a cut on the peak in TAC curve are listed in Tab. 2.

The majority of coincident γ-lines occurs as consequence of interactions of neutrons, backscattered from the target, with the detectors.

3.4. Neutron resonances

The integral time-of-flight spectrum is presented in the left part of Fig. 2. In there three characteristic regions are indicated, (I) γ-flash, (II) resonance region and (III) far delayed non-resonant region below the lowest resonance at 6.671 eV.

Calibration of TOF curve yields the list of observed neutron resonances. Resonances important for class-II states: 173.18 eV and 721.58 eV are not observed due to long dead system time after γ-flash. Summed γ-ray spectrum from all four detectors with the gate on 6.671 eV resonance compared to background spectrum is shown on Fig. 3.

4. Conclusions

The purpose of the presented feasibility study was to test functionality of the present setup and to provide us with guidance on how to improve it. Several important conclusions can be drawn. First, it is necessary to install properly designed shielding against different background components. The most deteriorating impact comes from the γ-flash during neutron production. Due to the proximity of our measurement laboratory to the neutron target hall, the intensity of the γ-flash is high. It extends the detector dead time, preventing us from reaching the interesting part of the TOF spectrum in ^{238}U. As a consequence of the long decay time of HPGe preamplifiers ($\approx$ 50 μs), all other pulses sum with γ-flash pulse, which leads to lower resolution, distorted peak shape and peak shifting. The energy distribution

Table 2. Coincident spectrum between detectors 3 and 4.

No	Energy(keV)	FWHM(keV)	Net count	Identification
1	272.7	2.07	157	^{115}In(n, γ)
2	324.9	1.08	192	^{70}Ge(n, γ)+^{72}Ge(n, γ)
3	416.8	2.13	508	^{115}In(n, γ)
4	478.7	0.89	692	^{10}B$(n, \alpha)^7$Li
5	492.9	1.87	145	^{73}Ge(n, γ)
6	500.1	2.62	245	^{70}Ge(n, γ)
7	511.2	3.87	2303	ANN
8	558.8	1.02	80	^{113}Cd(n, γ)
9	595.9	2.37	2519	^{73}Ge(n, γ)
10	608.5	1.99	416	^{73}Ge(n, γ)
11	701.5	0.93	104	^{73}Ge(n, γ)
12	708.3	1.08	134	^{70}Ge(n, γ)
13	818.8	0.63	82	^{115}In(n, γ)
14	867.9	3.07	852	^{73}Ge(n, γ)
15	960.7	2.07	189	^{73}Ge(n, γ)
16	1000.8	0.58	73	^{234m}Pa
17	1096.8	2.18	243	^{115}In(n, γ) +^{70}Ge(n, γ)+^{70}Ge(n, γ)
18	1203.6	2.24	187	^{73}Ge(n, γ)
19	1293.4	2.18	396	^{115}In(n, γ)
20	2223.3	1.69	277	^{1}H$(n, \gamma)d$

of γ-flash is rather broad, centered around 250 keV (Plompen et al., 2010). A good compromise for attenuation of as much of γ-flash radiation as possible and non-attenuation of neutron flux would be 2 cm lead shield installed close to the neutron production target well behind the wall.

Another source of background are neutrons, present even with closed shutter on the flight path. They amount to about 15% of neutrons in the interesting energy range, but carry no timing information. Neutron induced radiation in the accelerator wall results in many γ-lines in all parts of the spectrum. These background components could be treated by graded shield consisting of a moderator (such as paraffin or polyethylene), a neutron absorber (made from material with high capture cross section) and a γ-shielding (typically lead). If placed close to the detector, lead can serve also as a shield against environmental radiation.

Usefulness of coincident spectrum would be significantly enhanced if additional shield from target-scattered neutrons is placed in front of the detectors. Low-Z, low density material with high neutron scattering cross-section is ideal.

Transition from analog to digital data acquisition would further improve the setup. It would allow to employ pulse shape analysis to further suppress the impact of the γ-flash.

References

Canberra, http://www.canberra.com/products/detectors/pdf/REGe-Detector-SS-C40432.pdf

EUFRAT, Special Support Action, 7th Framework Programme of the European Atomic Energy Community, Nov. 1 (2008) to Oct. 31 (2012)

Oberstedt S. and Gunsing F. 1998. Evidence for low-energy γ-decay above the shape isomer in ^{239}U. Nucl. Phys. A 636, 129-138.

Oberstedt A., Oberstedt S., Gawrys M. and Kornilov N. 2007. Identification of a shape Isomer in ^{235}U. Phys. Rev. Lett. 99, 042502.

Ortec, http://www.ortec-online.com/Solutions/RadiationDetectors/semiconductor-photon-detectors.aspx

Ene, D et al., Nucl. Inst. Method A618 (2010) 54.

Send GmbH, Hamburg (2000).

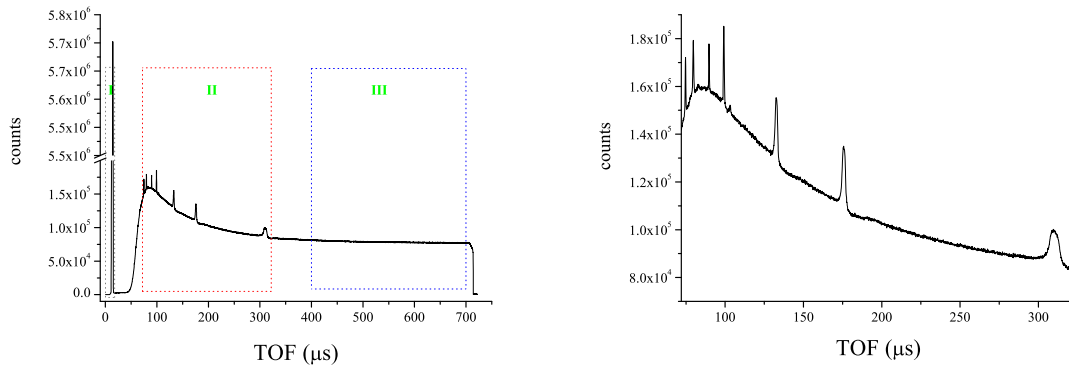Singh B., Zywina R. and Firestone R.B. 2002. Nuclear Data Sheets 97, 241.

Fig. 2. Left part: TOF spectrum with marked regions: I - γ-flash region, II - resonant region and III - far delayed region and; Right part: zoom into region II
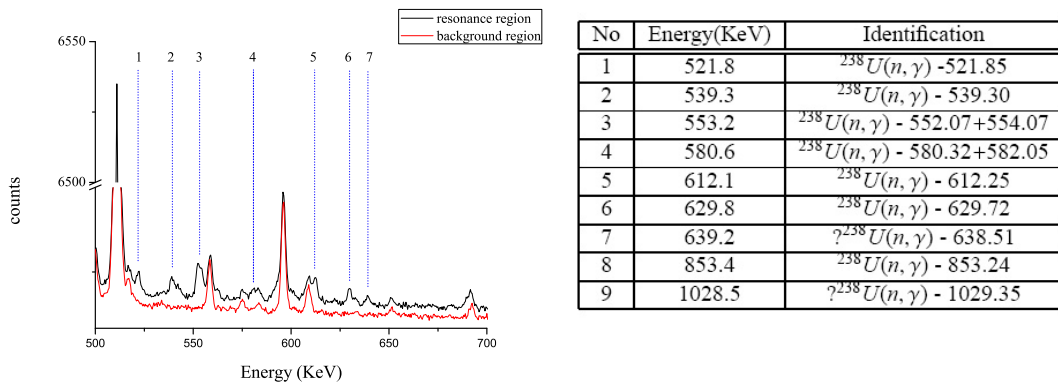

No	Energy(KeV)	Identification
1	521.8	$^{238}U(n, \gamma)$ -521.85
2	539.3	$^{238}U(n, \gamma)$ - 539.30
3	553.2	$^{238}U(n, \gamma)$ - 552.07+554.07
4	580.6	$^{238}U(n, \gamma)$ - 580.32+582.05
5	612.1	$^{238}U(n, \gamma)$ - 612.25
6	629.8	$^{238}U(n, \gamma)$ - 629.72
7	639.2	$?^{238}U(n, \gamma)$ - 638.51
8	853.4	$^{238}U(n, \gamma)$ - 853.24
9	1028.5	$?^{238}U(n, \gamma)$ - 1029.35

Fig. 3. Right part: the identified γ-lines from neutron capture in ^{238}U in the resonant region not visible in the non-resonant TOF region; Left part: Identified γ-lines in ^{239}U as indicated in the spectrum shown to the left.

Strutinsky V.M., 1967.Shell effects in nuclear masses and deformations energies. Nucl. Phys. A 95, 420-442.